Pulmonary Codelivery of Doxorubicin and siRNA by pH-Sensitive Nanoparticles for Therapy of Metastatic Lung Cancer

Caina Xu, Ping Wang, Jingpeng Zhang, Huayu Tian, Kinam Park, and Xuesi Chen**

***A** pulmonary codelivery system that can simultaneously deliver doxorubicin (DOX) and Bcl2 siRNA to the lungs provides a promising local treatment strategy for lung cancers. In this study, DOX is conjugated onto polyethylenimine (PEI) by using* cis*-aconitic anhydride (CA, a pH-sensitive linker) to obtain PEI-CA-DOX conjugates. The PEI-CA-DOX/siRNA complex nanoparticles are formed spontaneously via electrostatic interaction between cationic PEI-CA-DOX and anionic siRNA. The drug release experiment shows that DOX releases faster at acidic pH than at pH 7.4. Moreover, PEI-CA-DOX/Bcl2 siRNA complex nanoparticles show higher cytotoxicity and apoptosis induction in B16F10 cells than those treated with either DOX or Bcl2 siRNA alone. When the codelivery systems are directly sprayed into the lungs of B16F10 melanoma-bearing mice, the PEI-CA-DOX/Bcl2 siRNA complex nanoparticles exhibit enhanced antitumor efficacy compared with the single delivery of DOX or Bcl2 siRNA. Compared with systemic delivery, most drug and siRNA show a long-term retention in the lungs via pulmonary delivery, and a considerable number of the drug and siRNA accumulate in tumor tissues of lungs, but rarely in normal lung tissues. The PEI-CA-DOX/Bcl2 siRNA complex nanoparticles are promising for the treatment of metastatic lung cancer by pulmonary delivery with low side effects on the normal tissues.*

1. Introduction

Lung cancer represents a principal cause of cancer mortality worldwide.[1–3] The 5-year survival rate for lung cancer is for only 15%, and the majority of lung cancer patients survive for about 2 years.[4,5] The lung is a frequent site of metastasis organ, and greater than 90% of deaths are attributed to the metastatic process of lung cancer.[5,6] Despite the improvements in surgical techniques, chemotherapy, and radiation therapy, there are still big challenges to improve the survival rate for the patients with metastatic lung cancers.[7,8] It is desirable to develop improved therapeutic strategies for the treatment of metastasis lung cancers.

A major hurdle in lung cancer treatment is the low delivery efficiency and high side effect by traditional intravenous administration.[9,10] An attractive method to deal with this problem is to directly deliver drugs to the lungs via pulmonary administration.[11] Pulmonary delivery systems have advantages, including high concentrations of drugs in lung tumor tissues quickly, avoiding first-pass hepatic metabolism with reduced systemic side effects, and improved efficacies.[12–15] In addition, the lung tissue has a relatively large surface area that can absorb drugs effectively and prolong the retention of the delivered drugs in the lungs.[16] Currently,

Dr. C. Xu, P. Wang, J. Zhang, Prof. H. Tian, Prof. X. Chen
Key Laboratory of Polymer Ecomaterials
Changchun Institute of Applied Chemistry
Chinese Academy of Sciences
5625 Renmin Street, Changchun 130022, China
E-mail: thy@ciac.ac.cn; xschen@ciac.ac.cn
Prof. K. Park
Departments of Biomedical Engineering and Pharmaceutics
Purdue University
West Lafayette, IN 47907, USA
DOI: 10.1002/smll.201501034

www.MaterialsViews.com

some chemotherapies via pulmonary delivery for treatment of lung cancer are in clinical study.[17–19] The pulmonary administration has promising prospects for practical applications in lung cancer therapy.

It is well known that, doxorubicin (DOX) could cause DNA and RNA damage through inhibiting the ongoing of the topoisomerase II, thus induce the cell apoptosis.[20] Moreover, Bcl2 is a key regulator among the antiapoptotic proteins, which was found in the mitochondrial outer membrane and related to the mitochondrial pathway of apoptosis.[21] Codelivery of DOX and Bcl2 siRNA therapy using the same carrier to tumor cells would achieve synergistic or combining effects.[22,23] The combination of chemotherapy drug and gene is an effective method for cancer treatment, and researchers have developed a number of codelivery systems, with the advantages of synergistic function, overcoming drug resistance and reducing the side effects of drugs.[24,25] There are relevant reports using the codelivery systems for pulmonary administration. Porous microparticles (e.g., poly(lactic-*co*-glycolic acid)) for pulmonary delivery as powder formation have been shown to be a promising delivery system for the codelivery of drug and gene.[26] The cationic liposome carriers were successfully constructed for drug and gene codelivery system, and their therapeutic effect by pulmonary administration was more effective than that by intravenous administration.[27,28] The same group also developed silica nanospheres with similar results.[29] There have been few reports for the codelivery systems based on polymer nanoparticles for pulmonary delivery to simultaneously deliver chemotherapy drug and gene for treatment of lung cancers.

B16F10 melanoma cells are well established for metastatic lung cancer via tail vein, and the massive metastatic tumors in lungs are produced with only 2–3 weeks.[30] The main purpose of this study is to prepare the polymer nanoparticles for codelivery of DOX and siRNA by pulmonary administration for treatment of metastatic lung cancer (B16F10). In the present study, a chemotherapy drug, DOX, was conjugated to a commonly used polymeric gene carrier, polyethylenimine (PEI), by pH-sensitive linker to form a polymer-drug conjugate, which then formed complex nanoparticles with Bcl2 siRNA by electrostatic interactions. The codelivery system could be sprayed directly into the lungs. Subsequently, DOX and Bcl2 siRNA were codelivered to cancer cells for therapeutic effects (**Scheme 1**). The properties of the codelivery system were studied, including the complex particle sizes, zeta potential, drug release kinetics, cellular uptake, cell apoptosis, and cytotoxicity in vitro. The complex nanoparticles coloaded with DOX and Bcl2 siRNA were directly sprayed into the lungs by pulmonary administration, and the inhibition efficiency of metastatic lung cancers was evaluated. Moreover, the distributions of drug and siRNA in organs and tissues were characterized.

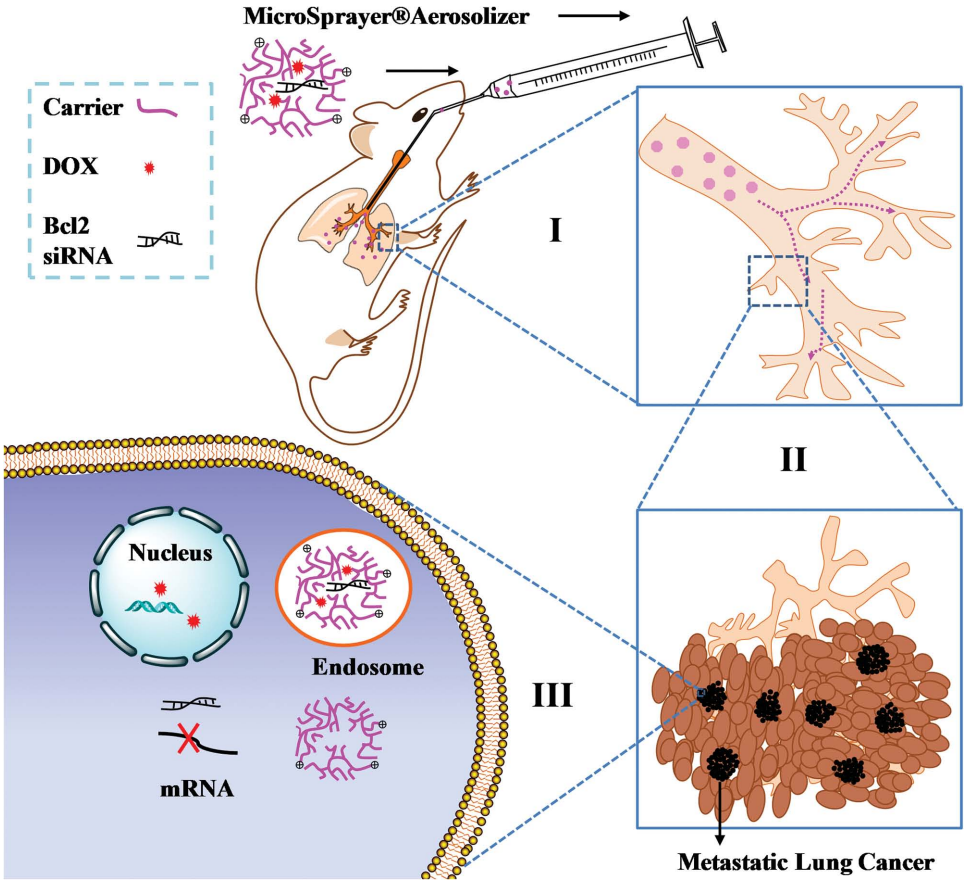

Scheme 1. Schematic illustration of pulmonary codelivery of DOX and siRNA to the lung. I,II) DOX and siRNA entered into trachea, bronchi, and alveolus; III) DOX and siRNA were codelivered to cancer cells.

small 2015,
DOI: 10.1002/smll.201501034

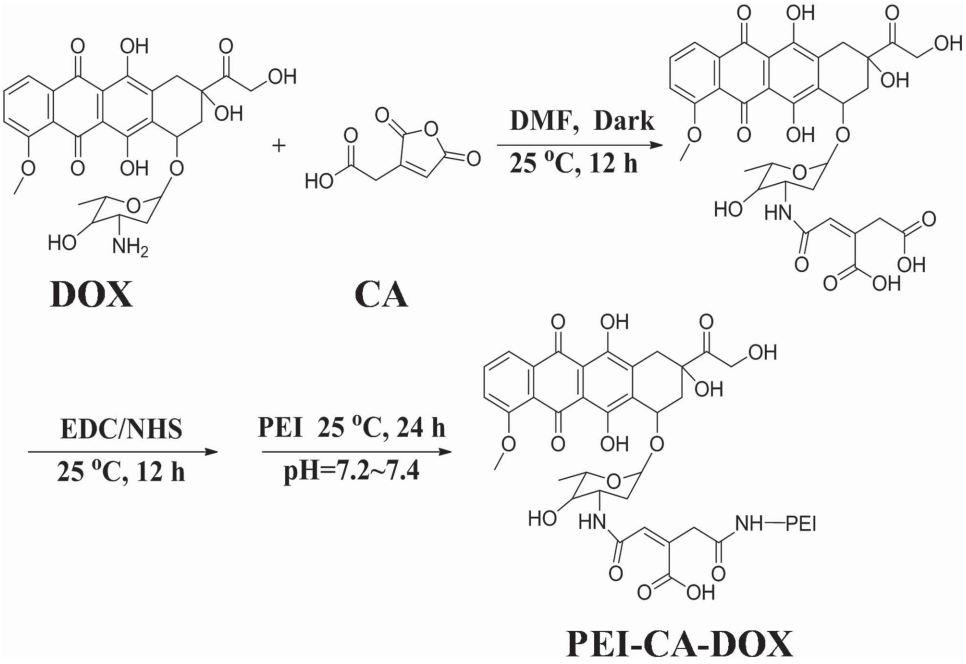

Figure 1. Synthesis procedures of PEI-CA-DOX.

2. Results and Discussion

2.1. Synthesis of PEI-CA-DOX and Characterization

The synthesis routes of PEI-CA-DOX are shown in **Figure 1**. The ^{1}H NMR spectra of PEI-CA-DOX are shown in **Figure 2**. In the ^{1}H NMR spectra of PEI-CA-DOX, the peaks of PEI are observed in 2.5–3.5 ppm,[31] and the peaks appeared at 7.0–8.0 ppm are assigned to DOX (a, b, c in Figure 2).[32] The ^{1}H NMR results exhibited that DOX with *cis*-aconitic anhydride (CA) linker was successfully conjugated to PEI. The DOX contents (%) of PEI-CA-DOX were 10.2% according to the ^{1}H NMR spectra, and this is consistent with the UV–vis spectrophotometry analysis at 485 nm (data not shown).

2.2. Drug Release Experiment

The DOX release from PEI-CA-DOX conjugate in phosphate buffer saline (PBS) solution was investigated at pH 5.0, 6.8,

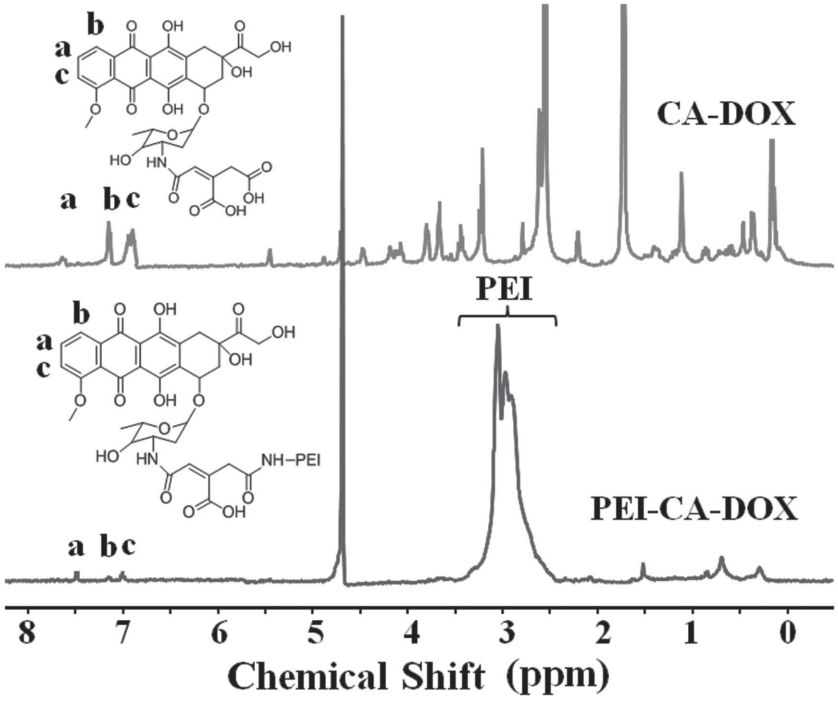

Figure 2. ^{1}H NMR spectra of PEI-CA-DOX in D_2O.

DOI: 10.1002/smll.201501034

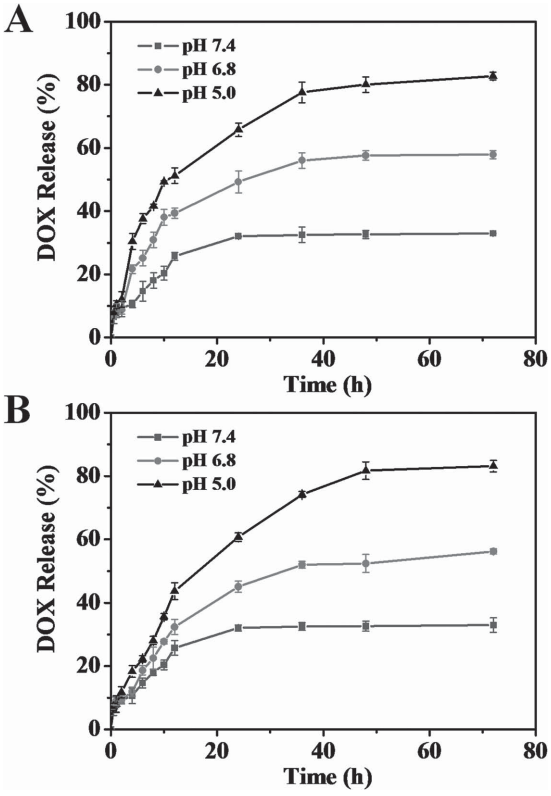

Figure 3. DOX release profiles for A) PEI-CA-DOX and B) PEI-CA-DOX/siRNA in PBS at pH 5.0, 6.8, and 7.4. Results are expressed as mean ± standard deviation ($n = 3$).

and 7.4. As shown in **Figure 3**, the release behaviors of DOX from PEI-CA-DOX and PEI-CA-DOX/DNA are both time- and pH-dependent. The release profiles of DOX showed that no significant initial burst was observed within 24 h and DOX displayed a fast release pattern at first followed by much slower release. The DOX release reached a relative plateau at a similar incubation time (about 36 h) at different pH values. After 72 h incubation, there was ≈30% of DOX released at physiological pH (pH 7.4), about 60% at pH 6.8, and greater than 80% at pH 5.0. Drug release under acidic conditions was higher than that under physiological conditions (pH 7.4), which was due to the cleavage of the pH-sensitive *cis*-aconityl linkage of PEI-CA-DOX under acidic conditions.[33]

2.3. Zeta Potential and Particle Size Analysis

The zeta potential of the PEI/siRNA and PEI-CA-DOX/siRNA complex nanoparticles (5/1, w/w) are +22.6 ± 1.7 mV and +18.3 ± 1.2 mV, respectively, which can increase cellular internalization by a nonspecific electrostatic interactions between the positively charged complex nanoparticles and negatively charged cell surface proteoglycans.[34] The particle size of PEI/siRNA (5/1, w/w) is 92.0 nm (**Figure 4**A). However, the particle size of PEI-CA-DOX/siRNA (5/1, w/w) is 76.0 nm (Figure 4B), which will be beneficial for tissue penetration. Previous researches have suggested that the size of the complex nanoparticles strongly affects their cellular uptake efficiency.[35] And the size of nanoparticles is also responsible for tumor accumulation.[36]

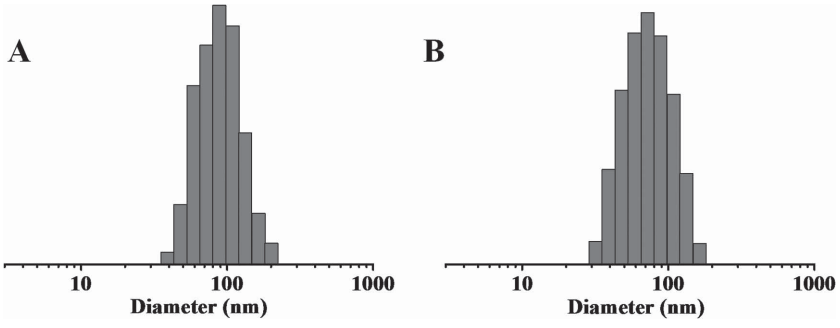

Figure 4. Particle sizes of A) PEI/siRNA and B) PEI-CA-DOX/siRNA at a ratio of 5/1 (w/w).

2.4. Cell Uptake Studies

To investigate the cellular internalization of DOX and siRNA, B16F10 cells were incubated with PEI-CA-DOX/Cy5 siRNA complex nanoparticles for 3 or 24 h and then examined with confocal laser scanning microscopy (CLSM). As shown in **Figure 5**, the blue fluorescence was from cell nucleus stained with 4′-6-diamidino-2-phenylindole (DAPI). The green fluorescence dots were induced from Cy5-labeled siRNA, and the red fluorescence spots were from DOX itself. At 3 and 24 h, both the green fluorescence dots and the red fluorescence spots were obviously observed in B16F10 cells, indicating that the codelivery system could simultaneously deliver siRNA and DOX into the same cells. The intracellular green fluorescence dots were diffusely distributed in cytoplasm at 3 and 24 h, which could be beneficial for the siRNA to silence the target gene in the cells. However, as the time extended from 3 to 24 h, with increasing cellular uptake, more DOX fluorescence could be observed in the cell nucleus. The results showed that more DOX cleaved from PEI-CA-DOX/siRNA nanoparticles in an acidic environment of endosomes and lysosomes.[37] In addition, the small-molecule DOX easily diffused into cell nucleus, and DOX induced DNA damage in the cell nucleus, thus exerted its cell apoptosis effects. The data were also consistent with in vitro release of DOX in buffered solutions. Furthermore, most of the DOX was located outside the endolysosomal regions (Figure S1A, Supporting Information). The obvious escape of siRNA from endolysosome was also observed in the cytoplasm which was proved by the obvious separation of red dots and green dots (Figure S1B, Supporting Information). Overall, these results indicated that both DOX and siRNA could be codelivered into cells with high efficiency, and might play different roles in the antitumor therapies.

2.5. Bcl2 Gene Silencing In Vitro

The downregulation of Bcl2 using small RNA interference technology has been considered as a potential therapeutic

DOI: 10.1002/smll.201501034

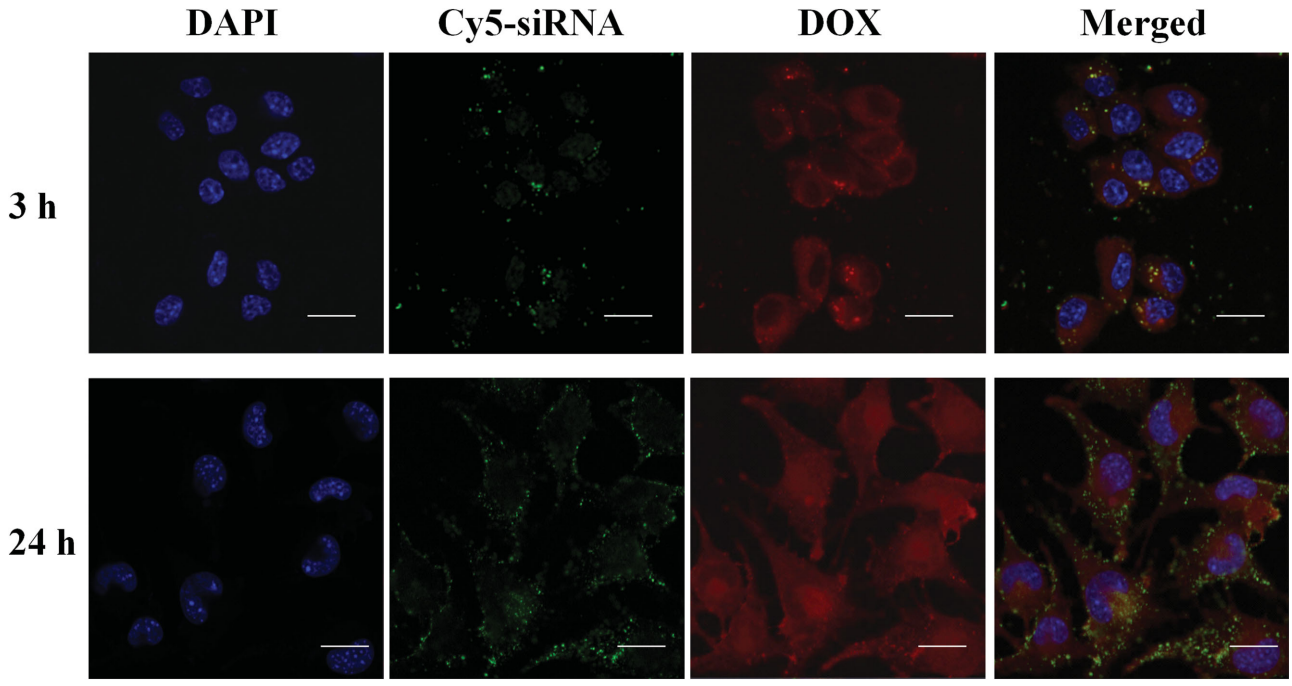

Figure 5. Cellular uptake of PEI-CA-DOX/siRNA complex nanoparticles in B16F10 cells incubated for 3 and 24 h, observed by confocal laser scanning microscopy. Cell nuclei were stained with DAPI (blue). The green fluorescence dots were induced from Cy5-labeled siRNA, and the red spots were from DOX itself. White scale bars = 20 μm.

option for anticancer therapy.[38,39] The Bcl2 gene silencing effect was determined by Bcl2 mRNA levels using quantitative real-time polymerase chain reaction (qRT-PCR). As shown in **Figure 6**, the PEI/Bcl2 siRNA induced a 74% decrease of Bcl2 mRNA, whereas cells incubated with the naked Bcl2 siRNA exhibited no significant difference at Bcl2 mRNA levels compared with the cells without treatment in control group. Thus, the results indicated that the PEI/Bcl2 siRNA could be efficiently delivered into B16F10 cells, and showed high gene silencing efficiency at the targeted mRNAs.

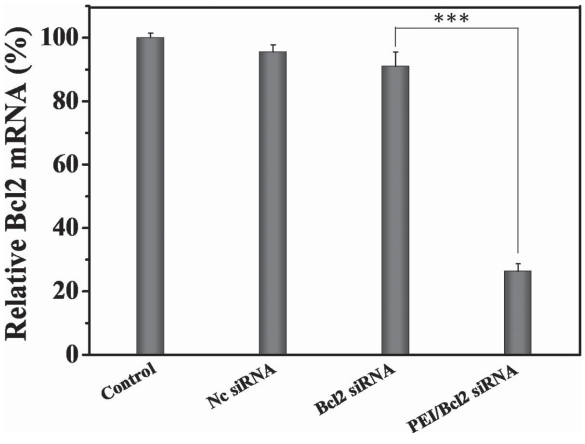

Figure 6. Effect of suppressing Bcl2 gene expression using Nc siRNA, Blc2 siRNA, and PEI/Bcl2 siRNA in B16F10 cells. β-actin as housekeeping gene was used for relative quantification. Data are shown as mean ± SD ($n = 3$). (***$P < 0.001$).

2.6. Cell Apoptosis

Cellular apoptosis induced by DOX and Bcl2 siRNA was measured by Annexin V-FITC staining assay.[40] As shown in **Figure 7**, the control cells without treatment exhibited a relatively low rate of apoptosis (8.3%). Furthermore, the cells incubated with PEI/Bcl2 siRNA, free DOX, and PEI-CA-DOX/Nc siRNA were induced 28.2%, 47.4%, and 46% apoptosis, respectively. Interestingly, much higher apoptotic rate (64.2%) was found in the cells treated with PEI-CA-DOX/Bcl2 siRNA than those only with siRNA (35.9% higher) or DOX (18.1% higher). These results demonstrated that DOX and Bcl2 siRNA could inhibit growth of B16F10 cells by inducing the cell apoptosis.

2.7. Cytotoxicity Assay

The cytotoxicity of PEI-CA-DOX/Bcl2 siRNA complex nanoparticles against B16F10 cells was measured in comparison to PEI/Bcl2 siRNA and PEI-CA-DOX/Nc siRNA nanoparticles using the 3-(4,5-dimethyl-2-thiazolyl)-2, 5-diphenyl-2-H-tetrazolium bromide (MTT) assay. As shown in **Figure 8** and Figure S2A,B (Supporting Information), compared with PEI/Bcl2 siRNA (containing therapeutic siRNA), free DOX (containing DOX only), and PEI-CA-DOX/Nc siRNA (containing DOX and negative control siRNA (Nc siRNA)), the cytotoxicity of PEI-CA-DOX/Bcl2 siRNA (containing DOX and Bcl2 siRNA) increased significantly at the same concentration (DOX 0.5 μg mL^{-1}, siRNA 1 μg mL^{-1}). These results demonstrate that the codelivery system of PEI-CA-DOX/Bcl2 siRNA can achieve higher

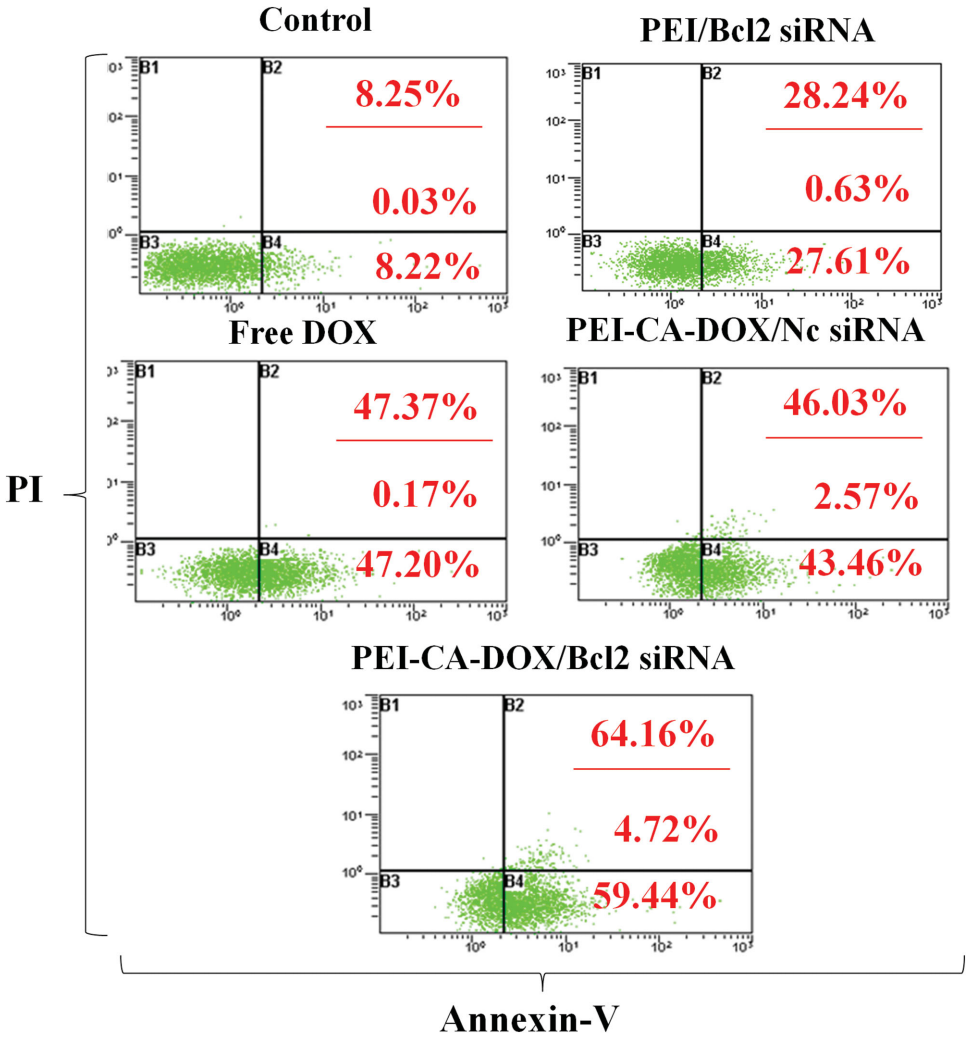

Figure 7. Evaluation on the apoptosis of B16F10 cells treated with PEI/Bcl2 siRNA, free DOX, PEI-CA-DOX/Nc siRNA, and PEI-CA-DOX/Bcl2 siRNA nanoparticles, respectively, for 48 h by flow cytometry.

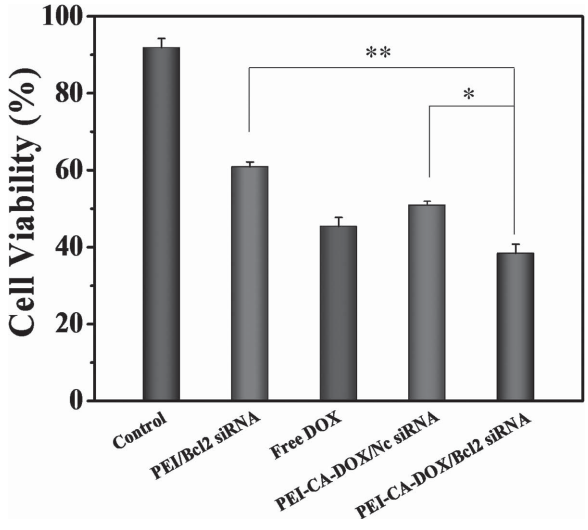

Figure 8. In vitro cell viability of B16F10 cells following incubation with PEI/Bcl2 siRNA, free DOX, PEI-CA-DOX/Nc siRNA, and PEI-CA-DOX/Bcl2 siRNA nanopaticles for 48 h, respectively. Indicated values are mean ± SD ($n = 6$). (*$P < 0.05$, **$P < 0.01$).

tumor cell inhibition effects at the same DOX dosage compared with monodelivery systems (PEI/Bcl2 siRNA, PEI-CA-DOX/Nc siRNA).

2.8. In Vivo Antitumor Therapy

The antitumor efficacy of drug and Bcl2 siRNA was investigated through the treatment of the metastatic lung cancer on C57BL/6 mice. During the animal experiment, the body weight of each mouse was measured every 3 d (Figure S3, Supporting Information), and there were no obvious changes in body weight among all the groups, implying the safety of the treatment method and delivery system type. **Figure 9** showed the photographs of lungs obtained from C57BL/6 mice in different treatment groups and control group. The lungs of B16F10 melanoma-bearing mice treated with PBS group displayed quite a number of melanoma nodes, and almost the whole lungs were occupied by tumors. However, the lungs of mice treated with monodelivery system or codelivery system showed less tumor nodes to some extent compared with PBS group. Significantly, the lungs excised from

DOI: 10.1002/smll.201501034

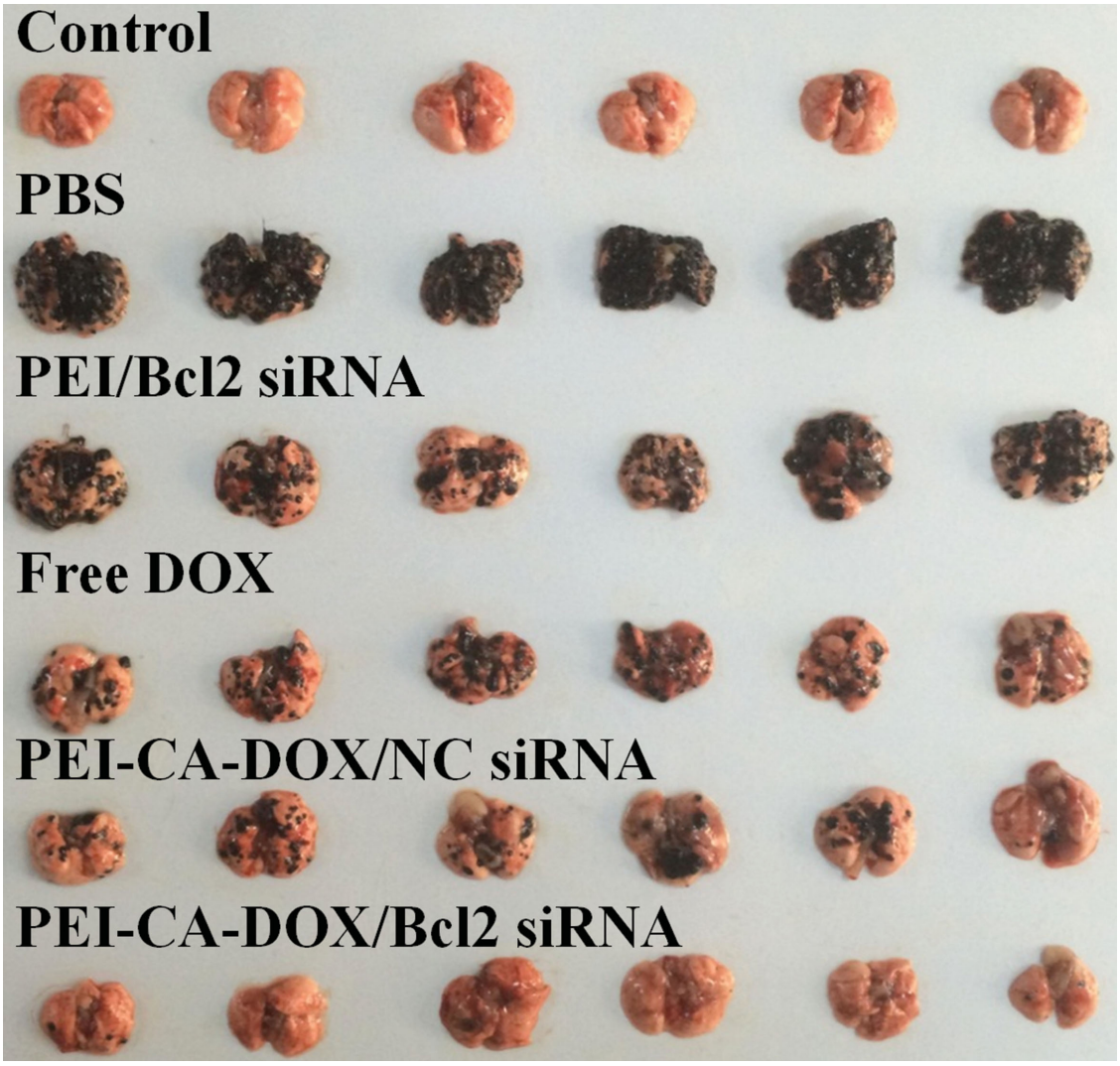

Figure 9. Photographs of lungs obtained from C57BL/6 mice. Control group represents the healthy lungs of mice without B16F10 cell implantation ($n = 6$), and other groups represent the lungs status of mice with B16F10 cell implantations via pulmonary administration of PBS, PEI/Bcl2 siRNA nanopartilces, free DOX, PEI-CA-DOX/Nc siRNA nanoparticles, and PEI-CA-DOX/Bcl2 siRNA nanoparticles, respectively, ($n = 6$).

PEI-CA-DOX/Bcl2 siRNA group were similar with control group, and tumors almost disappeared, which demonstrated that the codelivery DOX and Bcl2 siRNA by pulmonary delivery had synergistic antitumor efficacy.

The average lung weight of mice in each group was determined (**Figure 10**), which was associated with the weight of tumors. The average lung weight of mice treated with monodelivery system or codelivery system was significantly lower than that treated with PBS only (788.2 ± 70.4 mg). And the mice treated with codelivery DOX and Bcl2 siRNA showed the lowest lung weight (219.5 ± 20.3 mg) among all the treated groups and their lung weight were nearest to the healthy lung weight in control group (254.2 ± 42.8 mg). The therapeutic effects caused by codelivery system were significantly higher than free DOX and PEI/Bcl2 siRNA. The efficient antitumor effects were attributed to the combination of DOX and Bcl2 siRNA. And it was worthy to note that very low dose of DOX could obtain effective antitumor therapies after combination with Bcl2 siRNA by pulmonary administration. Only 30 μg DOX (10 μg each for three times) was administered during the treatment. However, previous studies reported that the doses of DOX for treating lung tumors were 200 μg (DOX only) and 40 μg (DOX and gene combination) by pulmonary administration,[26,41] and more doses of DOX were used when using intravenous injection.[42,43] Our results suggested that the drug dose for effective tumor inhibition could be achieved by combinational use of DOX and Bcl2 siRNA through pulmonary administration, which would be benefit to reduce the systemic toxicity, improve the safety of chemotherapeutics, as well as avoid the drug resistance.

2.9. Histological Examination

To further assess the antitumor efficacy treated with various formulations via pulmonary delivery, the sections of lung specimens were stained by hematoxylin and eosin (H&E) staining for pathology analysis. **Figure 11**A showed the lung sections observed by microscopy under low and high magnifications, respectively. The lung tissue sections of PBS treatment

DOI: 10.1002/smll.201501034

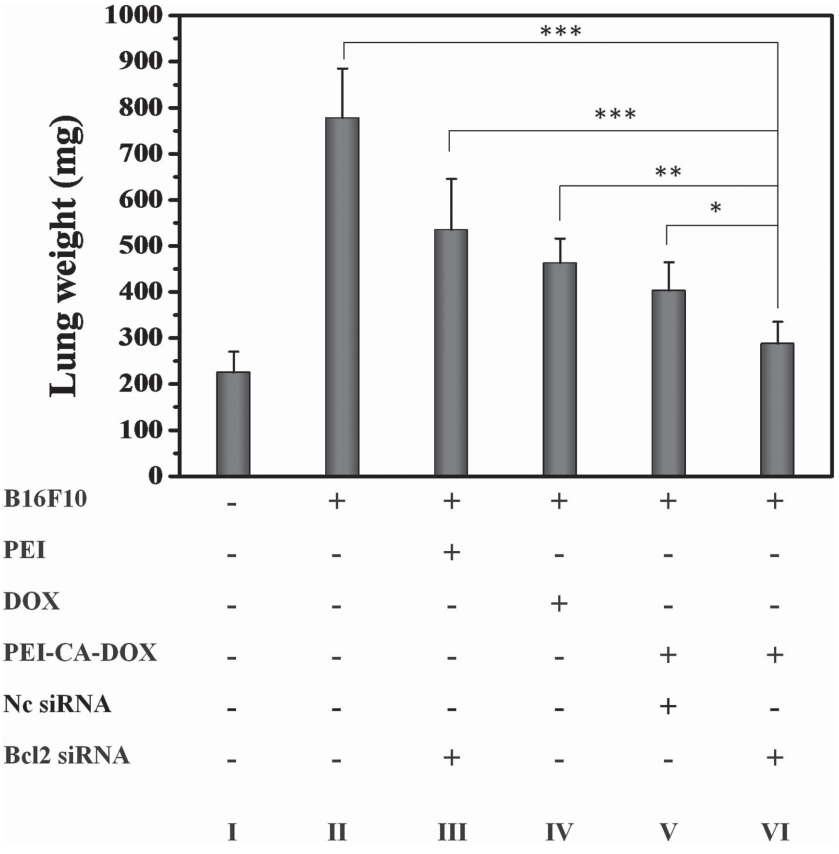

Figure 10. Average lung weights obtained from C57BL/6 mice. I) Control, II) B16F10 implanted and pulmonary PBS administered, III) B16F10 implanted and pulmonary PEI/Bcl2 siRNA nanoparticles administered, IV) B16F10 implanted and pulmonary free DOX administered, V) B16F10 implanted and pulmonary PEI-CA-DOX/Nc siRNA nanoparticles administered, VI) B16F10 implanted and pulmonary PEI-CA-DOX/Bcl2 siRNA nanoparticles administered (*$P < 0.05$, **$P < 0.01$, ***$P < 0.001$).

showed many melanomas, and visible pigmentation could be observed in the sections. The lungs of mice treated with drug or Bcl2 siRNA showed obvious reductions in tumor mass and numbers and exhibited many normal pores. Especially, the lung specimens of mice treated with codelivery of drug and Bcl2 siRNA showed typical pores, like in the lung specimen of nontreated negative control, indicating that the codelivery complex nanoparticles (PEI-CA-DOX/Bcl2 siRNA) performed the most effective antitumor effects among all the treatment groups. In addition, some representative sections were detected to verify the organ damage, including the heart, liver, spleen, and kidney (Figure 11B). The histological analysis of mice showed that the main tissues of mice treated by pulmonary administration exhibited no significant morphological changes compared with the control group, which further conformed to the safety of pulmonary delivery.

2.10. Biodistribution

The DOX and siRNA distributions in different organs were observed by in vivo imaging system at different time points. PEI-CA-DOX/Cy5 siRNA nanoparticles, free DOX, and free Cy5 siRNA were delivered into mice by two administration methods, pulmonary and systemic administration. As shown in **Figure 12**A, after systemic delivery, free DOX was mainly distributed in the livers and kidneys. It was noticeable that the free DOX exhibited high fluorescence intensity in the liver until 48 h after systemic delivery, which is due to the reticuloendothelial system.[44] After pulmonary administration of free DOX, the DOX fluorescence in the lungs was much higher than that in systemic administration, and gradually weakened after 48 h. However, the lungs treated with PEI-CA-DOX/Cy5 siRNA nanoparticles by pulmonary administration could not only possess higher red fluorescent intensity in lungs compared with systemic administration but also induce strong fluorescence intensity until 7 d (Figure 12B), indicating that most of the administered PEI-CA-DOX was deposited in the lung to improve therapeutic effect. Furthermore, in vivo distributions of free Cy5 siRNA and PEI-CA-DOX/Cy5 siRNA complex nanoparticles were also observed after pulmonary or systemic administration (Figure 12C,D). The results were similar to the DOX fluorescence intensity distribution. The images in Figure 12 suggest that pulmonary delivery could induce higher DOX and siRNA concentrations in the lungs compared with systemic delivery. And compared with free siRNA, PEI-CA-DOX/Cy5 siRNA complex nanoparticles could cause longer retention time in lungs. For free DOX and siRNA, they are easily metabolized in a short period of time, or siRNA may be easily degraded in vivo.[45] After loaded in nanoparticles, DOX and siRNA could be protected and gradually released to achieve longer retention time compared with the free DOX and siRNA. The results demonstrated that pulmonary administration of nanocarriers resulted in higher DOX and siRNA concentrations and longer retention time in lungs.

2.11. Intracellular Uptake of DOX and siRNA In Vivo

To further evaluate the distribution of DOX and siRNA in lung tissues and tumors when they were loaded in PEI-CA-DOX/siRNA complex nanoparticles, CLSM was used to observe the sections of the lungs from mice 24 h after pulmonary or systemic administration of PEI-CA-DOX/siRNA complex nanoparticles. As shown in **Figure 13**, the blue regions are the cell nucleus stained with DAPI, the red dots are fluorescent from DOX, and the green spots are the fluorescence of Cy5 labeled siRNA. White arrows and dotted lines point the tumor regions. There were no obvious DOX and Cy5 fluorescence in lung tissues of the mice by systemic administration of PEI-CA-DOX/siRNA complex nanoparticles. This may be due to excretion of the

DOI: 10.1002/smll.201501034

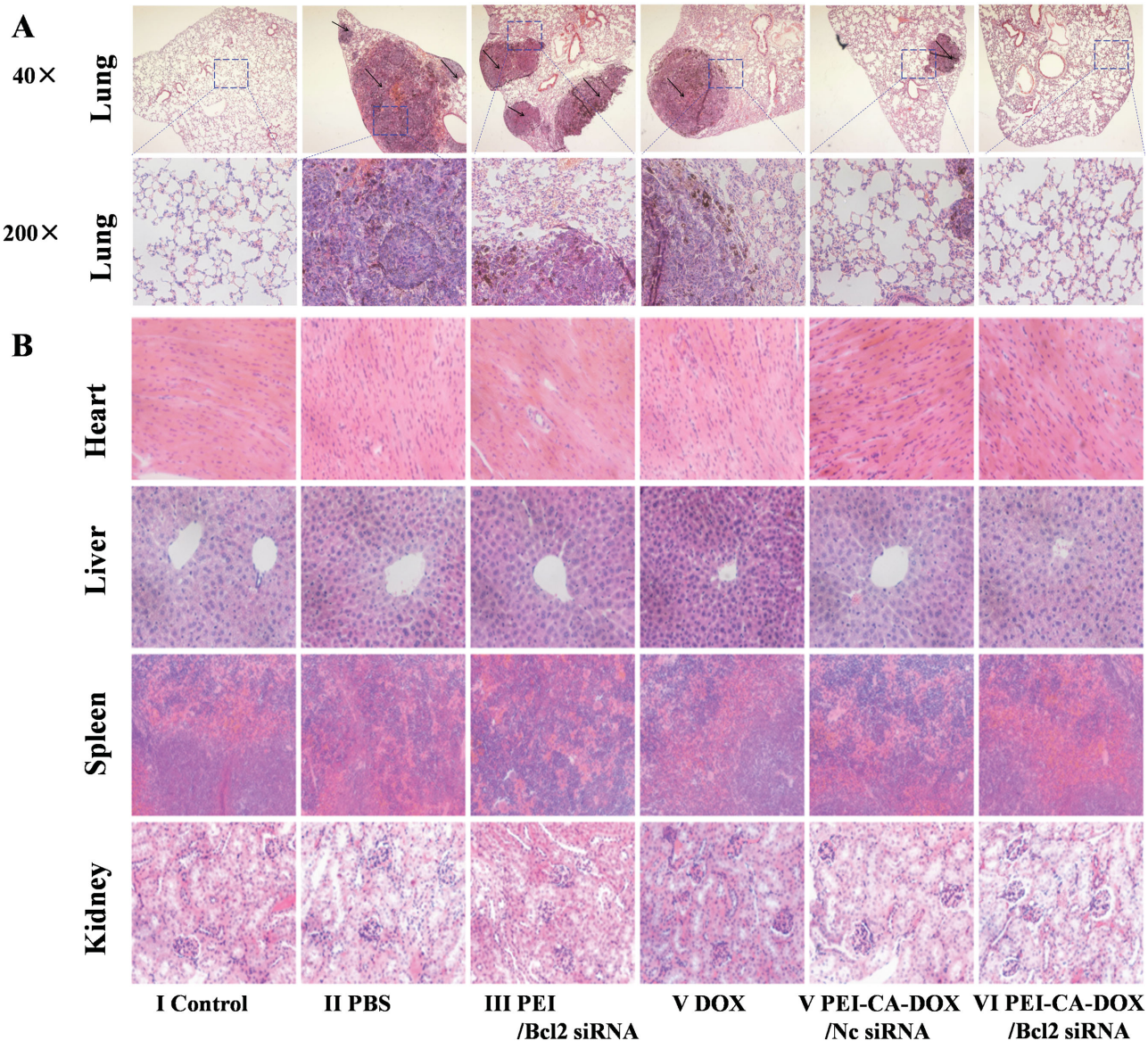

Figure 11. A) Histological sections of lung tissues were observed by microscopy under low (40×) and high (200×) magnifications. B) Histological sections of heart, liver, spleen, and kidney organs of C57BL/6 mice after different treatments were examined under (100×) magnification. I) Control, II) B16F10 implanted and pulmonary PBS administered, III) B16F10 implanted and pulmonary PEI/Bcl2 siRNA nanoparticles administered, IV) B16F10 implanted and pulmonary free DOX administered, V) B16F10 implanted and pulmonary PEI-CA-DOX/Nc siRNA nanoparticles administered, VI) B16F10 implanted and pulmonary PEI-CA-DOX/Bcl2 siRNA nanoparticles administered. Black arrows indicated the tumor tissues.

majority of drug and gene from the body within 24 h. This phenomenon is in accordance with the results in Figure 12. In contrast, sections of lungs delivered by pulmonary administration of PEI-CA-DOX/siRNA complex nanoparticles showed strong fluorescent intensity of DOX or Cy5 in the tumor tissues, indicating that the considerable amount of DOX and siRNA was aggregated in tumor tissues in the lungs, but rarely in normal lung tissues. Though pulmonary administration belongs to the local delivery method, the nanoparticles could also access the pulmonary circulation system after pulmonary administration. Because of the defective blood vessels and the lack of lymphatic circulation system in tumor tissues, the PEI-CA-DOX/siRNA complex nanoparticles tended to accumulate in tumor tissues in the lungs.[37,46] In addition, the tumor tissues are rich in blood vessels,[47] which might lead to higher DOX and siRNA concentrations in the tumor areas.

3. Conclusion

In this study, PEI-CA-DOX/siRNA complex nanoparticles were successfully constructed for pulmonary delivery. Importantly, the complex nanoparticles had suitable size and zeta potential for endocytosis, favorable drug release profiles, apoptosis induction, and high cytotoxicity in B16F10 cells. Furthermore, the pulmonary codelivery of DOX and siRNA significantly inhibited the tumor growth in metastatic lung cancer models in mice with low side effects due to increased concentrations of DOX and Bcl2 siRNA, prolonged residence time in

www.MaterialsViews.com

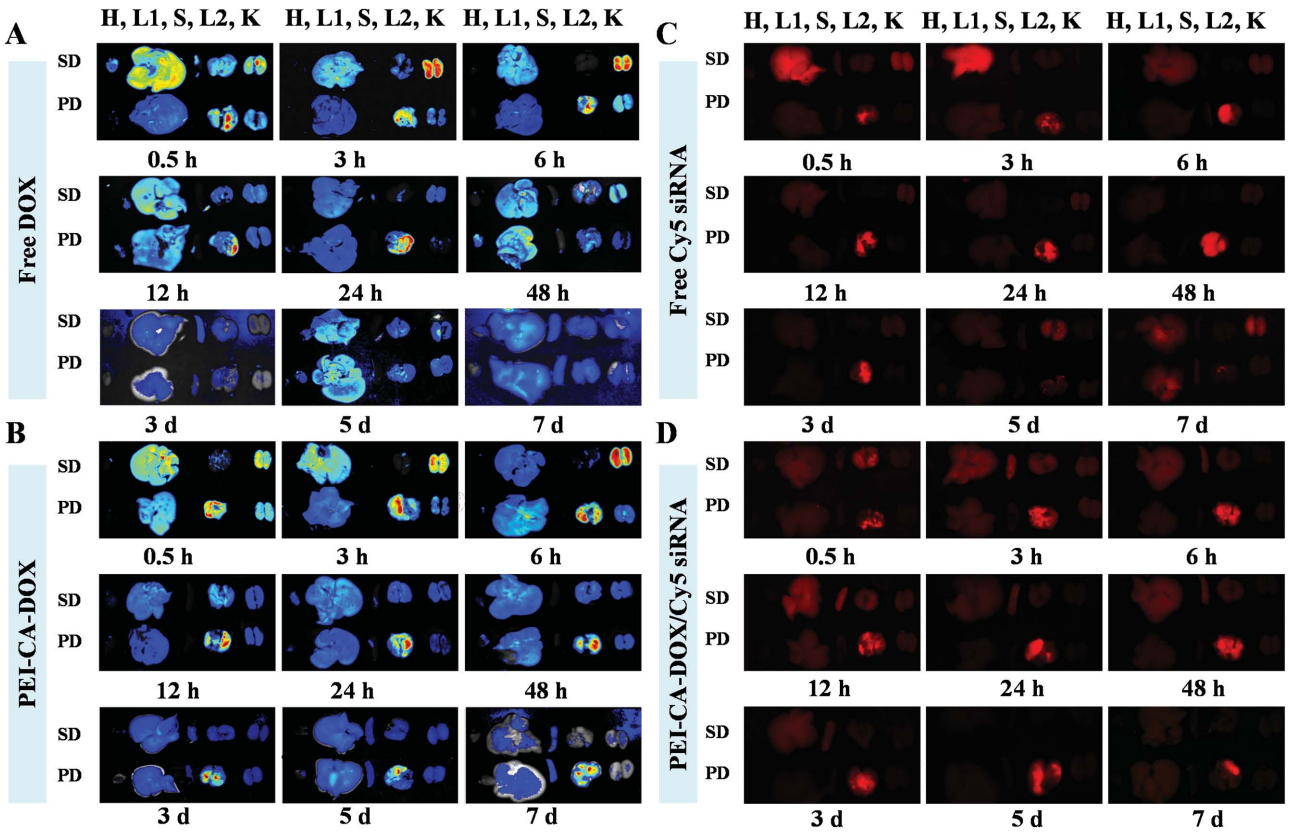

Figure 12. Distribution of DOX and Cy5 labeled siRNA in the lungs and other main organs (H, heart; L1, liver; S, spleen; L2, lung; K, kidney). Organ distribution by observing DOX fluorescence for free A) DOX and B) PEI-CA-DOX in mice at 0.5 h, 3 h, 6 h, 12 h, 24 h, 48 h, 3 d, 5 d, and 7 d after systemic delivery (SD) and pulmonary delivery (PD). Organ distribution by observing siRNA fluorescence for free Cy5 labeled siRNA C) and PEI-CA-DOX/Cy5 labeled siRNA D) in mice at 0.5 h, 3 h, 6 h, 12 h, 24 h, 48 h, 3 d, 5 d, and 7 d after systemic delivery (SD) and pulmonary delivery (PD).

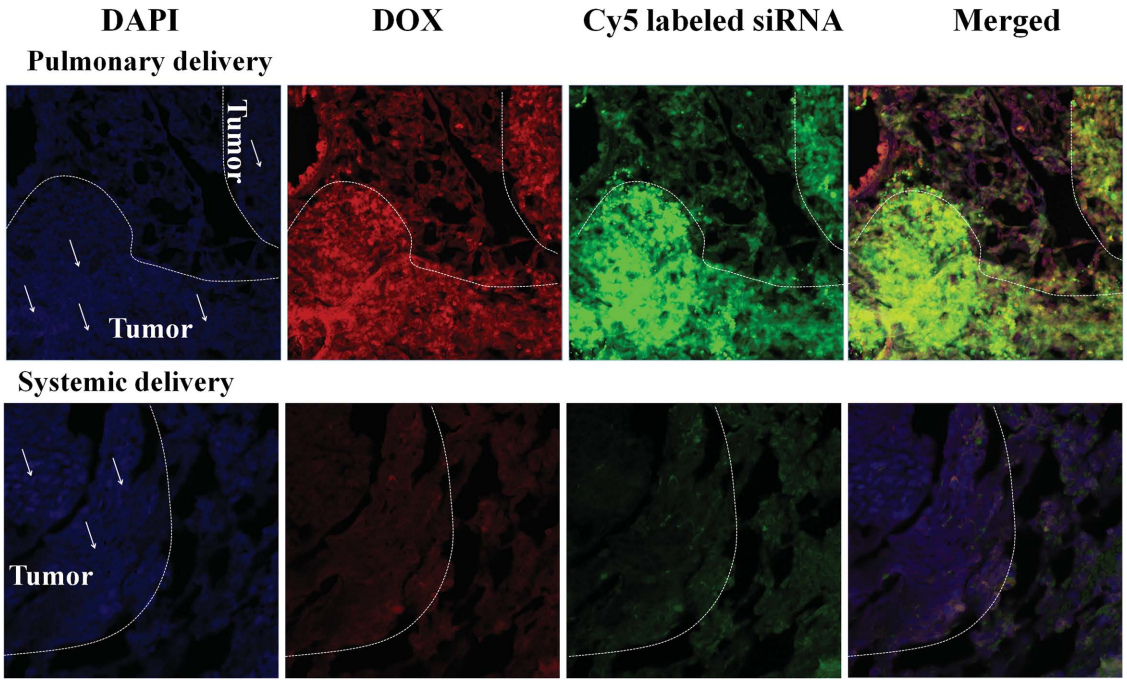

Figure 13. Accumulation of DOX and Cy5 labeled siRNA in tumor tissue and normal lung tissue following the pulmonary delivery (top) systemic delivery (bottom) of the PEI-CA-DOX/siRNA complex nanoparticles at 24 h. Lung sections were observed under CLSM. The cell nuclei were stained by DAPI (blue). DOX is in red color, and Cy5 labeled siRNA is in green color. White arrows and dotted lines are pointed to the tumor areas.

small 2015,
DOI: 10.1002/smll.201501034

lungs, and resulting increased accumulation in the tumor tissues in lungs. Our findings indicate that pulmonary delivery of PEI-CA-DOX/Bcl2 siRNA complex nanoparticles is a treatment strategy to consider for the metastatic lung cancer treatment.

4. Experimental Section

Reagents and Materials: Branched polyethyleneimine (PEI, molecular weight of 25 000 Da) was purchased from Sigma-Aldrich (St. Louis, MO, USA). Doxorubicin hydrochloride (DOX HCl) was purchased from Beijing Huafeng United Technology Co., Ltd. (Beijing, China). Dulbecco's modified Eagle medium, trypsin-ethylene diamine tetraacetie acid (EDTA) solution, and fetal bovine serum were purchased from Gibco (Grand Island, USA). Two Bcl-2 siRNA duplexes (Bcl2-1 and Bcl2-2) and negative control siRNA (Nc siRNA) were purchased from Genepharma (Suzhou, China) with the sequences as follows: Bcl2-1 siRNA (sense) 5′-UGU GGA UGA CUG AGU ACC UGAdTdT-3′, (antisense) 5′-UCA GGU ACU CAG UCA UCC ACAdTdT-3′; Bcl2-2 siRNA (sense) 5′-GUA CAU CCA UUA UAA GCU GUCdTdT-3′, (antisense) 5′-GAC AGC UUA UAA UGG AUG UACdTdT-3′, Nc siRNA (sense) 5′-UUC UCC GAA CGU GUC ACG UTTdTdT-3′, (antisense) 5′-ACG UGA CAC GUU CGG AGA ATTdTdT-3′. The mixture of Bcl2-1 siRNA and Bcl2-2 siRNA in equal molar ratio was called Bcl2 siRNA. Cy5-labeled negative siRNA was purchased from RiboBio (Guangzhou, China). PrimeScript RT Master Mix and SYBR Premix Ex Taq were purchased from Takara Biotechnology Co., Ltd. (Dalian, China). Other reagents were analytical grade and purchased from Beijing Chemical Works (Beijing, China).

Synthesis of PEI-CA-DOX and Characterization: PEI-CA-DOX conjugate was synthesized as follows. DOX (50.0 mg) and *cis*-aconitic anhydride (CA, 59.2 mg) was dissolved in 10 mL of anhydrous dimethylformamide. The solution was stirred for 24 h at room temperature in the dark. The formed CA-DOX was lyophilized. Then, CA-DOX was dissolved in dimethyl sulfoxide (DMSO) followed by drop-wise addition of N-Hydroxysuccinimide (NHS) and 1-Ethyl-3-(3-Dimethylaminopropyl)Carbodiimide (EDC) for 12 h. The solution was drop-wise added to the PEI solution (pH = 7.2–7.4) and stirred for 24 h at room temperature in the dark. Following dialysis and lyophilization, PEI-CA-DOX conjugate was obtained and stored at 4 °C for later use. The chemical structures of PEI-CA-DOX conjugate were characterized by ^{1}H NMR at 400 MHz (Bruker, Ettlingen, Germany) in D_2O.

Preparation of PEI/siRNA and PEI-CA-DOX/siRNA: PEI or PEI-CA-DOX and siRNA were suspended in deionized water, and PEI/siRNA or PEI-CA-DOX/siRNA complex nanoparticles were prepared at a 5/1 (w/w) ratio followed with gently vortexing. After incubation at room temperature for 30 min, PEI/siRNA and PEI-CA-DOX/siRNA complex nanoparticles were obtained.

Drug Release Experiment: PEI-CA-DOX or PEI-CA-DOX/DNA was diluted into 2 mL PBS of different pH values (5.0, 6.8, and 7.4) at a concentration equivalent to 50.0 μg mL^{-1} free DOX and put into a dialysis bag (MWCO 7000 Da). Calf thymus DNA was used as the substitute for siRNA. The dialysis bag was immersed in 58 mL of PBS container at 37 °C for 72 h with continuous shaking. At the regular time points, 2 mL of PBS from container was removed for testing and 2 mL fresh PBS was added into the container. Excitation and emission wavelengths of 480 nm and 590 nm were applied for the detection of DOX concentration. The cumulative release of DOX was calculated and the results were presented as mean ± standard deviation.

Particle Sizes and Zeta Potential Analysis: The particle sizes and zeta potential of the PEI/siRNA or PEI-CA-DOX/siRNA complex nanoparticles suspended in deionized water were determined by a zeta potential/BI-90Plus particle size analyzer (Brookhaven, USA).

Cell Uptake Studies: Intracellular localization of PEI-CA-DOX/siRNA complex nanoparticles in B16F10 cells was investigated using confocal laser scanning microscopy (CLSM, ZEISS LSM 780, Germany). The siRNA was labeled with fluorescent dye Cy5. B16F10 cells (1×10^5 cells/well) were seeded into 6-well plates and incubated for 24 h. Then, PEI-CA-DOX/siRNA (5/1, w/w, 2.0 μg of siRNA/well) complex nanoparticles were added into each well. After incubation for 24 h, cells were rinsed with PBS five times and fixed with 4% paraformaldehyde for 15 min at room temperature. The nuclei were stained with 4′-6-diamidino-2-phenylindole (DAPI, 1 mg mL^{-1}) for 2 min. The coverslips were placed on slides and enclosed in glycerol before exposing to CLSM.

Quantification of Bcl2 Gene Expression by qRT-PCR: B16F10 cells seeded in 6-well plates at 1×10^5 cells/well were treated with Nc siRNA, Bcl2 siRNA, or PEI/Bcl2 siRNA (5/1, w/w, 2.0 μg of siRNA/well) for 48 h. The total mRNA was extracted from cells using the Trizol reagent (Invitrogen). The cDNA was synthesized using reverse transcription kit from Takara Biotechnology Co., Ltd. (Dalian, China). Quantitative real-time PCR using PrimeScript RT Master Mix and SYBR Premix Ex Taq was carried out by Mxpro 3005P Real-Time PCR Detection system (Stratagene, USA). The real-time PCR program was performed at the initial heating at 95 °C for 10 min, 40 cycles of 95 °C for 30 s, 56 °C for 1 min, and 72 °C for 1 min. The primers for Bcl2 were as follows: forward, 5′-AGG AGC AGG TGC CTA CAA GA-3′; reverse, 5′-GCA TTT TCC CAC CAC TGT CT-3′. For β-actin: forward, 5′-TGT TAC CAA CTG GGA CGA CA-3′; Reverse, 5′-GGG GTG TTG AAG GTC TCA AA-3′.

Cell Apoptosis: B16F10 cells (2×10^5 cells/well) were seeded on 6-well plates and incubated overnight. After the treatment with PEI/Bcl2 siRNA (5/1, w/w, 2.0 μg of siRNA/well), free DOX (0.5 μg mL^{-1}), PEI-CA-DOX/Nc siRNA (5/1, w/w, 2.0 μg of siRNA/well), and PEI-CA-DOX/Bcl2 siRNA (5/1, w/w, 2.0 μg of siRNA/well) for 48 h, the cells were rinsed with cold PBS and then trypsinized for 1 min before collection. Afterward, the cells were resuspended in binding buffer and stained with Annexin V-FITC and propidium iodide using apoptosis analysis kit (Invitrogen). The apoptosis of B16F10 cells was monitored on a flow cytometer (BD, USA).

Cytotoxicity Assay: The cytotoxicities of nanoparticles against B16F10 cells were evaluated by MTT assay. The cells were seeded into 96-well plates at 1×10^4 cells/well and cultured at 37 °C in a 5% CO_2 atmosphere overnight. PEI/Bcl2 siRNA (5/1, w/w, 0.2 μg of siRNA/well), free DOX (0.5 μg mL^{-1}), PEI-CA-DOX/Nc siRNA (5/1, w/w, 0.2 μg of siRNA/well), and PEI-CA-DOX/Bcl2 siRNA (5/1, w/w, 0.2 μg of siRNA/well) were added into each well in replicates of six and incubated for 12, 24, and 48 h, respectively. Subsequently, 20 μL of MTT (5 mg mL^{-1}) was added into each well and incubated for extra 4 h. Finally, each well was added with 160 μL of DMSO and measured at 492 nm using a Bio-Rad 680 Microplate Reader. Cell viability (%) was calculated as the following equation

$$\text{Cell viability (\%)} = (A_{\text{sample}}/A_{\text{control}}) \times 100\% \quad (1)$$

where A_{sample} represents the absorbencies of the sample wells and A_{control} represents the absorbencies of control wells.

DOI: 10.1002/smll.201501034

In Vivo Antitumor Therapy: All animal experiments were cared for in accordance with the guidelines for laboratory animals established by the School of Life Sciences Animal Care and Use Committee of Northeast Normal University. Male C57BL/6 mice (18–20 g) were injected with B16F10 cells (1×10^4 cells per mouse) through a tail vein to obtain an animal model of metastatic lung cancer. Tumor-bearing mice were randomly divided into six groups. The drug and siRNA (DOX 10 μg, siRNA 20 μg) were delivered directly to the lungs through pulmonary administration in aerosol form using a liquid aerosol device (MicroSprayer Aerosolizer, Penn-Century, Philadelphia, PA, USA). Pulmonary administration was performed according to a modification of the previously described procedure.[12] Mice were anesthetized by intraperitoneal injection of pentobarbital sodium (Sigma, USA) at dose of 70 mg kg^{-1} body weight. DOX and siRNA were directly delivered into the lungs of mice through intratracheal route three times at 3, 10, and 17 d after B16F10 cell implantation. After 24 d, the mice were sacrificed and the lungs were harvested. In addition, the body weight of each mouse was measured every 3 d.

Histological Examination: Lung specimens were fixed with paraformaldehyde (4%), embedded in paraffin, sectioned (5 μm) and stained with hematoxylin and eosin (H&E). The H&E stained pathological sections were examined by microcopy (Nikon TE2000U) under low and high magnification (40× and 200×), respectively. Histopathologies of other organs (heart, liver, spleen, and kidney) in each group were collected and stained with H&E to evaluate the safety by microscope.

Biodistribution: The PEI-CA-DOX/Cy5 siRNA (DOX 10 μg, siRNA 20 μg), free DOX (DOX 10 μg), and free Cy5 siRNA (siRNA 20 μg) were separately delivered by pulmonary administration or intravenous injection. The major organs (heart, liver, spleen, lung, and kidney) of mice at 0.5, 3, 6, and 12 h and at 1, 2, 3, 5, and 7 d postadministration were excised. After brief washing with physiological saline, the fluorescence distribution was visualized using a Maestro in vivo Imaging System (Cambridge Research & Instrumentation, Inc., USA) at excitation and emission wavelengths of 523 and 560 nm for DOX and of 650 and 670 nm for Cy5 siRNA, respectively. The distribution of DOX and Cy5 siRNA fluorescence in different organs was analyzed using a commercial software (Maestro 2.4).

Intracellular Uptake of DOX and siRNA In Vivo: To measure DOX and Cy5-siRNA distribution in normal tissues or tumor tissues, the PEI-CA-DOX/Cy5 siRNA complex nanoparticles (DOX 10 μg, siRNA 20 μg) were delivered via pulmonary administration or the intravenous injection. After 24 h, the mice were sacrificed and all the lungs were frozen at –80 °C overnight, and then sectioned into 5 μm/slice. The nuclei were stained by DAPI for 5 min and washed with cold PBS for 5 min. Finally, the slices were observed by CLSM.

Statistical Analysis: The data were shown as mean ± standard deviation. The statistical significance was analyzed using the Student's *t*-test. *P*-values of <0.05 were regarded as statistically significant. All experiments were repeated at least three times.

Supporting Information

Supporting Information is available from the Wiley Online Library or from the author.

Acknowledgements

The authors are thankful to the National Natural Science Foundation of China (Grant Nos. 51222307, 21474104, 51390484, 51233004, and 51321062), Jilin Province Science and Technology Development Program (20120306 and 20130521011JH), Open Research Fund of the Key Laboratory of Advanced Technologies of Materials, Ministry of Education, Southwest Jiaotong University, and Youth Innovation Promotion Association, CAS.

[1] R. Siegel, D. Naishadham, *CA Cancer J. Clin.* **2013**, *63*, 11.
[2] M. Malvezzi, P. Bertuccio, F. Levi, C. La Vecchia, E. Negri, *Ann. Oncol.* **2013**, *24*, 792.
[3] A. Jemal, M. J. Thun, L. A. Ries, H. L. Howe, H. K. Weir, M. M. Center, E. Ward, X. C. Wu, C. Eheman, R. Anderson, U. A. Ajani, B. Kohler, B. K. Edwards, *J. Natl. Cancer Inst.* **2008**, *100*, 1672.
[4] C. S. Dela Cruz, L. T. Tanoue, R. A. Matthay, *Clin. Chest Med.* **2011**, *32*, 605.
[5] M. Carballo, M. S. Maish, D. E. Jaroszewski, C. E. Holmes, *J. Cardiothorac. Surg.* **2009**, *4*, 13.
[6] H. Goto, S. Yano, H. L. Zhang, Y. Matsumori, H. Ogawa, D. C. Blakey, S. Sone, *Cancer Res.* **2002**, *62*, 3711.
[7] L. Crino, W. Weder, J. van Meerbeeck, E. Felip, *Ann. Oncol.* **2010**, *21*, v103.
[8] F. Al-Shahrabani, D. Vallbohmer, S. Angenendt, W. T. Knoefel, *J. Clin. Oncol.* **2014**, *5*, 595.
[9] J. Wong, A. Brugger, A. Khare, M. Chaubal, P. Papadopoulos, B. Rabinow, J. Kipp, J. Ning, *Adv. Drug Deliv. Rev.* **2008**, *60*, 939.
[10] M. Wacker, *Int. J. Pharm.* **2013**, *457*, 50.
[11] C. N. Xu, H. Y. Tian, X. S. Chen, *Chin. J. Chem.* **2014**, *32*, 13.
[12] M. Bivas-Benita, R. Zwier, H. E. Junginger, G. Borchard, *Eur. J. Pharm. Biopharm.* **2005**, *61*, 214.
[13] W. H. Roa, S. Azarmi, M. H. Al-Hallak, W. H. Finlay, A. M. Magliocco, R. Lobenberg, *J. Controlled Release* **2011**, *150*, 49.
[14] J. K. Lam, W. Liang, H. K. Chan, *Adv. Drug Deliv. Rev.* **2012**, *64*, 1.
[15] T. S. Feng, H. Y. Tian, C. N. Xu, L. Lin, Z. G. Xie, M. H. Lam, H. J. Liang, X. S. Chen, *Eur. J. Pharm. Biopharm.* **2014**, *88*, 1086.
[16] O. M. Merkel, M. Zheng, H. Debus, T. Kissel, *Bioconjugate Chem.* **2012**, *23*, 3.
[17] G. A. Otterson, M. A. Villalona-Calero, W. Hicks, X. Pan, J. A. Ellerton, S. N. Gettinger, J. R. Murren, *Clin. Cancer Res.* **2010**, *16*, 2466.
[18] G. A. Otterson, M. A. Villalona-Calero, S. Sharma, M. G. Kris, A. Imondi, M. Gerber, D. A. White, M. J. Ratain, J. H. Schiller, A. Sandler, M. Kraut, S. Mani, J. R. Murren, *Clin. Cancer Res.* **2007**, *13*, 1246.
[19] J. K. Watts, D. R. Corey, *Bioorg. Med. Chem. Lett.* **2010**, *20*, 3203.
[20] S. Aroui, S. Brahim, M. De Waard, A. Kenani, *Biochem. Biophys. Res. Commun.* **2010**, *391*, 419.
[21] R. J. Youle, A. Strasser, *Nat. Rev. Mol. Cell Biol.* **2008**, *9*, 47.
[22] N. Cao, D. Cheng, S. Y. Zou, H. Ai, J. M. Gao, X. T. Shuai, *Biomaterials* **2011**, *32*, 2222.
[23] M. Saad, O. B. Garbuzenko, T. Minko, *Nanomedicine* **2008**, *3*, 761.
[24] W. C. Chen, Y. Y. Yuan, D. Cheng, J. F. Chen, L. Wang, X. T. Shuai, *Small* **2014**, *10*, 2678.
[25] H. Meng, M. Liong, T. Xia, Z. Li, Z.X Ji, J. I. Zink, A. E. Nel, *ACS Nano* **2010**, *4*, 4539.
[26] I. Kim, H. J. Byeon, T. H. Kim, E. S. Lee, K. T. Oh, B. S. Shin, K. C. Lee, Y. S. Youn, *Biomaterials* **2013**, *34*, 6444.
[27] O. B. Garbuzenko, M. Saad, S. Betigeri, M. Zhang, A. A. Vetcher, V. A. Soldatenkov, D. C. Reimer, V. P. Pozharov, T. Minko, *Pharm. Res.* **2009**, *26*, 382.

DOI: 10.1002/smll.201501034

[28] O. B. Garbuzenko, M. Saad, V. P. Pozharov, K. R. Reuhl, G. Mainelis, T. Minko, *Proc. Natl. Acad. Sci. USA* **2010**, *107*, 10737.
[29] O. Taratula, O. B. Garbuzenko, A. M. Chen, T. Minko, *J. Drug Target.* **2011**, *19*, 900.
[30] Y. Y. Guan, X. Luan, J. R. Xu, Y. R. Liu, Q. Lu, C. Wang, H. J. Liu, Y. G. Gao, H. Z. Chen, C. Fang, *Biomaterials* **2014**, *35*, 3060.
[31] G. P. Tang, H. Y. Guo, F. Alexis, X. Wang, S. Zeng, T. M. Lim, J. Ding, Y. Y. Yang, S. Wang, *J. Gene Med.* **2006**, *8*, 736.
[32] F. Q. Hu, L. N. Liu, Y. Z. Du, H. Yuan, *Biomaterials* **2009**, *30*, 6955.
[33] X. W. Guan, Y. H. Li, Z. X. Jiao, J. Chen, Z. P. Guo, H. Y. Tian, X. S. Chen, *Acta Biomater.* **2013**, *9*, 7672.
[34] M. A. Mintzer, E. E. Simanek, *Chem. Rev.* **2009**, *109*, 259.
[35] S. Dufort, L. Sancey, J. L. Coll, *Adv. Drug Deliv. Rev.* **2012**, *64*, 179.
[36] V. Torchilin, *Adv. Drug Deliv. Rev.* **2011**, *63*, 131.
[37] S. J. Zhu, M. H. Hong, G. T. Tang, L. L. Qian, J. Y. Lin, Y. Y. Jiang, Y. Y. Pei, *Biomaterials* **2010**, *31*, 1360.
[38] D. Cheng, N. Cao, J. F. Chen, X. S. Yu, X. T. Shuai, *Biomaterials* **2012**, *33*, 1170.
[39] A. J. Garcia-Saez, *Cell Death Differ.* **2012**, *19*, 1733.
[40] I. Vermes, C. Haanen, H. Steffensnakken, C. Reutelingsperger, *J. Immunol. Methods* **1995**, *184*, 39.
[41] I. Kim, H. J. Byeon, T. H. Kim, E. S. Lee, K. T. Oh, B. S. Shin, K. C. Lee, Y. S. Youn, *Biomaterials* **2012**, *33*, 5574.
[42] P. F. Gou, W. W. Liu, W. W. Mao, J. B. Tang, Y. Q. Shen, M. H. Sui, *J. Mater. Chem. B* **2013**, *1*, 284.
[43] H. M. Liu, Y. Li, A. Mozhi, L. Zhang, Y. L. Liu, X. Xu, J. M. Xing, X. J. Liang, G. H. Ma, J. Yang, X. Zhang, *Biomaterials* **2014**, *35*, 6519.
[44] H. J. Cho, I. S. Yoon, H. Y. Yoon, H. Koo, Y. J. Jin, S. H. Ko, J. S. Shim, K. Kim, I. C. Kwon, D. D. Kim, *Biomaterials* **2012**, *33*, 1190.
[45] Y. Y. Huang, J. M. Hong, S. Q. Zheng, Y. Ding, S. T. Guo, H. Y. Zhang, X. Q. Zhang, Q. Du, Z. C. Liang, *Mol. Ther.* **2011**, *19*, 381.
[46] S. Biswas, V. P. Torchilin, *Adv. Drug Deliv. Rev.* **2014**, *66*, 26.
[47] L. Y. Joanne, J. W. Rak, G. Klement, R. S. Kerbel, *Cancer Res.* **2002**, *62*, 1838.

Received: April 14, 2015
Revised: May 31, 2015
Published online: